AIAA 80-0303R

Sonic Fatigue Design Data for Bonded Aluminum Aircraft Structures

Marcus J. Jacobson*
Northrop Corporation, Hawthorne, Calif.

A combined analytical and experimental program was conducted to determine sonic fatigue design properties of bonded structural sections commonly used in aircraft and to formulate data and criteria for the development of sonic fatigue designs of such structure. An objective of the program was to develop information applicable to aircraft fuselage panels using adhesive bonding in the primary structure, in lieu of mechanical fasteners such as are currently used. Ten flat, rectangular, acoustic test panels featuring the FM73/BR127 adhesive system, a phosphoric acid anodizing process, and 7075-T6 aluminum alloy skin and substructure were designed and fabricated. Panel tests were conducted under broadband acoustic excitation. In preliminary testing, nonlinear strain-pressure relationships were observed and natural frequencies increased with sound pressure level. Subsequently, sonic fatigue tests were conducted at a constant overall sound pressure level. The lives of the bonded panels were generally much greater than the sonic fatigue lives of riveted 7075-T6 aluminum alloy panels of comparable size and thickness. Based on the test data and theoretical considerations, a sonic fatigue design chart was developed. It is expected that the approach in developing the sonic fatigue design chart will remain applicable when different bonding systems and surface preparations are considered.

Nomenclature

a	= bay width (in.)
b	= bay length (in.)
c	= viscous damping factor
c_c	= critical viscous damping factor
dB	= Decibel (reference pressure 0.00002 N/m^2)
f_1	= fundamental frequency of panel response with low-level excitation (Hz)
f_{166}	= predominant response frequency at 166 dB SPL (Hz)
h	= panel (skin) thickness (in.)
M	= bending moment per unit length (in.-lb/in.)
N	= number of cycles
PSD	= power spectral density
S	= rms dynamic stress
SEM	= scanning electron microscope
S_P	= acoustic spectrum level (psi/Hz$^{1/2}$)
SPL	= sound pressure level (dB)
$\bar{\sigma}_S$	= skin stress parameter defined in Eq. (1)
σ'	= stress parameter defined in Eq. (2)
ζ	= nondimensional viscous damping factor = c/c_c

Introduction

BECAUSE of recent advances in bonding technology, considerable attention is being directed at developing design and manufacturing techniques that will permit the use of bonded metallic structure in significant applications in aircraft. The use of the Boeing Process Specification BAC-5555 has been shown to be a superior method for preparing the surfaces of aircraft aluminum alloys for bonding. Because of the expected use of bonded structure in sonic environments featuring the application of the BAC-5555 Process Specification or its equivalent, the need for sonic fatigue guidelines for the new generation bonded structures becomes evident.

Submitted Jan. 9, 1980; presented as Paper 80-0303 at the AIAA 18th Aerospace Sciences Meeting, Pasadena, Calif., Jan. 14-16, 1980; revision received Oct. 21, 1980.

*Senior Technical Specialist, Structural Dynamics Research Department, Aircraft Division. Member AIAA.

There is extensive information in the general literature[1-9] on sonic fatigue design data and approaches to guard against the sonic fatigue of riveted structures. However, the sonic fatigue data for riveted structures is not directly transferable to bonded structures, principally because of the different nature of the riveted joint assemblies vs bonded joint assemblies.

The program objective of the analytical and experimental activity[10] being reported in this paper was the determination of sonic fatigue properties of bonded structural sections based on skin-stringer-frame design commonly applied in aircraft and the formulation of data and criteria for the development of sonic fatigue-resistant designs for such structures. The surfaces of all the panels tested in this program were treated with a phosphoric acid anodizing process that complied with the BAC-5555 process specifications. The FM73/BR127 adhesive system was used in the bonding of the test specimens. The 7075-T6 aluminum alloy was selected for the skins and substructure of all the test specimens.

The test results obtained in this program were evaluated and used in the development of a semiempirical method for predicting the sonic fatigue lives of bonded multibay aircraft panels. The sonic fatigue lives of the bonded multibay test panels were, in general, significantly longer than the lives of multibay riveted aluminum alloy panels of comparable size and skin thicknesses.[10] It is expected that the approach in developing the sonic fatigue design chart for the bonded panels will be applicable when other bonding systems and surface preparation methods are considered.

Design and Fabrication of Acoustic Test Panels

The configurations of the acoustic test panels were chosen to be compatible with current and expected flight vehicle requirements. Ten cross-stiffened 9-bay panels (Table 1) were designed and manufactured for acoustic tests that were conducted in the 48- by 48-in. test section of Northrop's progressive wave acoustic test chamber (Fig. 1). The unstiffened side of a typical test panel is shown in Fig. 2 and the stiffened side of the same test panel is shown in Fig. 3.

The cross-stiffening elements of the 9-bay panels were 4.00-in. deep I-section members and 1.25-in. deep J-section members (Fig. 4) simulating fuselage frames and longerons, respectively. The flanges of the cross-stiffeners in contact with the skins of the test panels were scarfed to approximately

Table 1 Description of acoustic test panels

Panel design	Overall panel dimensions, in.	Central bay dimensions, in.	Skin thickness, in.
A-1	29×20	18×9	0.032
A-2	29×20	18×9	0.040
A-3	29×20	18×9	0.050
A-4	36×24	24×12	0.050
A-5	36×24	24×12	0.063

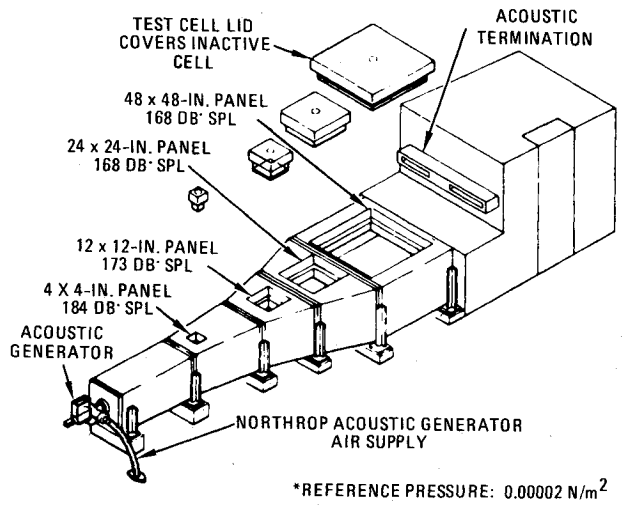

Fig. 1 Progressive wave acoustic chamber.

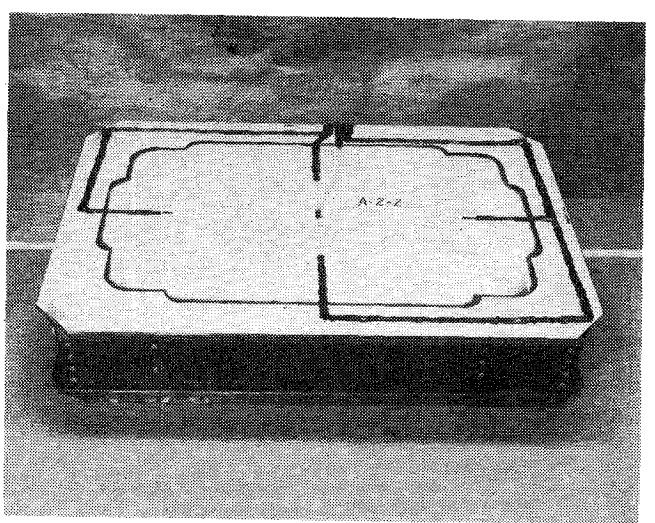

Fig. 2 Unstiffened side of panel A-2-2.

0.030 in. to reduce stress concentration effects at the ends of the bonded joints and hence to increase the sonic fatigue lives of the bonded joints. Angles were mechanically fastened to the web of the I-section members to simulate a flange on zee section components of frame section designs for production aircraft. Only the first acoustic test panel (Panel A-3-1) did not have the angle stiffeners installed on the I-section members, and this may have been a factor in the sonic fatigue failure that occurred in the joint between cross-stiffeners and through a portion of the J-section member.

The J-section members were continuous through cutouts in the I-section members. At the intersection of the J-section and I-section members, an angle clip was mechanically fastened to the cross-stiffeners to produce a joint.

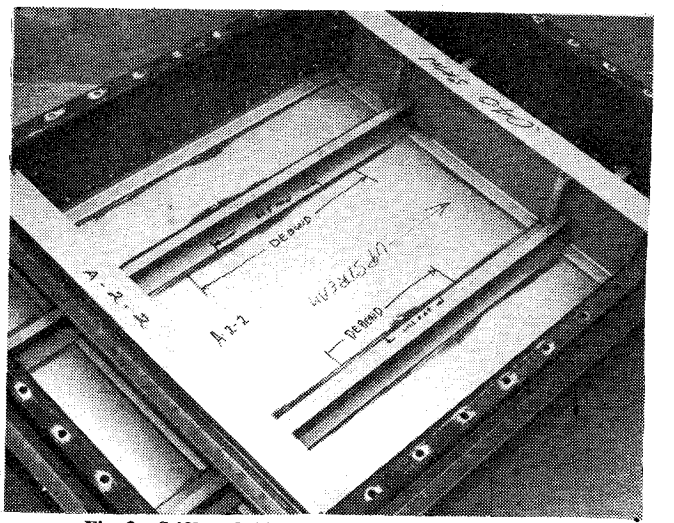

Fig. 3 Stiffened side of panel A-2-2 (after acoustic test).

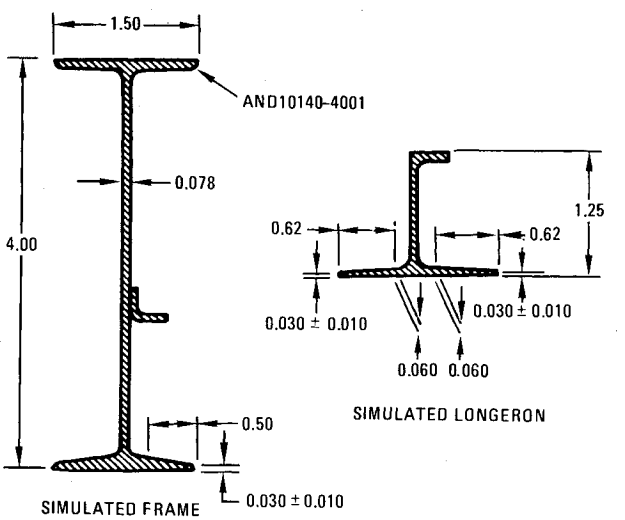

Fig. 4 Cross sections of substructural elements.

Two other test panel design features to be noted were the boundary frame (Figs. 2 and 3) and the edge doubler (Fig. 2). Functionally, the boundary frame and the edge doubler were a part of the test fixture. Thus, the test section of the multibay test panels was comprised of the central bay, the cross-stiffening elements that bounded the central bay and the bonded joints bounding the central bay. The remainder of the acoustic test panels (i.e., the other eight bays, the boundary frame and edge doubler) was designed to simulate typical aircraft structure that may bound the sonic fatigue test region of interest. Precautions were taken in the design of the edge doubler, boundary frame, and outer eight bays to guard against sonic fatigue failures in those regions which could have influenced the location and time of subsequent sonic fatigue failures in the region of interest and raised questions on the meaning of the test results.

The FM73/BR127 adhesive/primer system for 250F service temperature capability was used in this program to bond the skins of the acoustic test panels to the stiffeners that were simulating the aircraft internal structure. The unit weight of the FM73 supported film adhesive used in the manufacture of the acoustic test panels was 0.085 psf.

The metal surface preparation (for bonding) consisted of a phosphoric acid anodize treatment that conformed to the Boeing Process Specification BAC-5555. The phosphoric acid anodize treatment and the priming were performed in the Long Beach facility of McDonnell Douglas Aircraft Corporation by Douglas Aircraft Company personnel in ac-

cordance with the Douglas Process Standard (DPS) 11.08 and (DPS) 1.950 (Process Engineering Order D-001C). The primed parts were wrapped and delivered to Northrop where the bonding of the multibay panels took place. The cure procedure for bonding the panels is given in Ref. 10. Following the bonding, nondestructive inspection (NDI) was conducted on the bonded acoustic panel structure. The C-scan records provided evidence of satisfactory bonding. After the NDI inspection was performed, the remainder of the assembly of the test panels was completed.

Instrumentation and Testing

Acoustic signals and displacement probe indications were analyzed and recorded by a B&K, Type 3315, Audio Frequency Spectrum Recorder System. A Spectral Dynamics Real Time Analyzer (SD 301C) with its one-octave and 1/3-octave band converter, was also used to monitor the environment and the specimen responses.

The boundary frame of each acoustic test panel was mounted on a jig plate and installed in the 48- by 48-in. test cell of the progressive wave test chamber (Fig. 5). In addition, a 3 ft high termination box was fabricated and installed above the jig plate porting which leads to the stiffened side of the acoustic test panel. The termination box was constructed with 1 in. plywood and was lined internally with open cell polyurethane foam of 4 in. thickness.

Immediately prior to installing an acoustic test panel in the progressive wave test chamber for sonic fatigue testing, modal surveys were conducted on the panel to determine natural frequencies of the panel. A damping factor ζ was obtained for each of the acoustic test panels with the logarithmic decrement method, utilizing the oscillograph decay record taken from the strain gage signals under loudspeaker excitation and low-level discrete frequency testing in the progressive wave test chamber. All discrete frequency excitation was of short duration and sufficiently low level to avoid producing any appreciable fatigue damage to the panel specimen.

After the modal surveys were completed and damping factors were obtained under low-level discrete frequency excitation, the panel specimens were subjected to broadband acoustic loading at 136 dB overall sound pressure level (SPL), and strain data were recorded. The sound pressure level was increased in increments of 3 dB and data were recorded at each SPL until the level was reached for the sonic fatigue test. The SPL for the sonic fatigue test was the maximum SPL of the test cell and was 166 dB overall SPL. One purpose of the test procedure of increasing the SPL from 136 dB to the final level was to observe if nonlinear effects were present. The testing at SPL's lower than the maximum test SPL was conducted rapidly in order to prevent undue exposure before the intended fatigue test commenced.

Visual inspection was used as the primary determinant of fatigue failure. The visual inspections were conducted on a sliding schedule where the interval between inspections was related to accumulated test time. In addition, inspections were performed at any time in response to indicated changes noted in the response wave form or the spectral distribution of strain. Particular attention was given to tracking the predominant response frequency in the output of selected strain gages. The tests were halted once a fatigue crack was observed and recorded.

Sonic fatigue failures were obtained in the broadband acoustic tests of all ten 9-bay acoustic test panels. The locations and modes of sonic fatigue failures are shown in the schematic drawings of Fig. 6. The test lives are recorded in Table 2. All acoustic test panels except for panel A-3-1, which was the first acoustic panel tested, experienced bond failures. Panel A-3-1 experienced its sonic fatigue failure in a stiffener at a clip. The cycles to failure were calculated as the product of the predominant response frequency and the acoustic exposure time at 166 dB overall SPL.

The acoustic pressure spectrum levels during the 166 dB runs are given in Table 2 and are based on 1/3 octave band acoustic pressure data and in some cases on narrow band data at the beginning of the sonic fatigue testing at 166 dB. Spectrum level "A" in Table 2 is based on 1/3 octave band acoustic pressure data, whereas spectrum level "B" is based on narrow band acoustic pressure data. Inasmuch as all strain gages did not have the same frequency for the occurrence of the peak in the strain PSD, the use of the spectrum level based on the 1/3 octave band acoustic pressure is recommended.

A compilation of pertinent features of multibay panels tested under broadband acoustic loading in other programs was made and reported in Ref. 10. Most of the sonic fatigue test panels reviewed from other programs featured riveted joints between the skin and substructure. In general, the bonded panels listed in Table 2 were much more sonic fatigue-resistant than the other panels.

Panel A-5-1 was sectioned following the termination of the sonic fatigue test. Investigation of the sonic fatigue failure mode of panel A-5-1, with scanning electron microscope (SEM) analysis, resulted in the conclusion that there was cohesive failure in the primer near the 7075-T6 aluminum skin rather than adhesive failure at the surface of the skin. No other acoustic test panel was subjected to SEM analysis.

Modal and Damping Data

Under loudspeaker excitation with the panel mounted on the jig plate for the acoustic tests, the lowest natural frequency (f_1) was obtained for all acoustic test panels except panel A-3-1. The mode shape corresponding to the lowest natural frequency (Table 3) consisted of one-half wave in the width direction and one-half wave in the length direction of the central bay.

The ratio of the frequency at which the peak strain PSD occurred in the sonic fatigue test at 166 dB overall SPL to the fundamental frequency obtained under the loudspeaker excitation is f_{166}/f_1 in Table 3. This ratio is a measure of the panel stiffening resulting from the high-intensity noise excitation. The predominant response frequency at 166 dB overall SPL was obtained by tracking the low-level fundamental frequency through increasing levels.

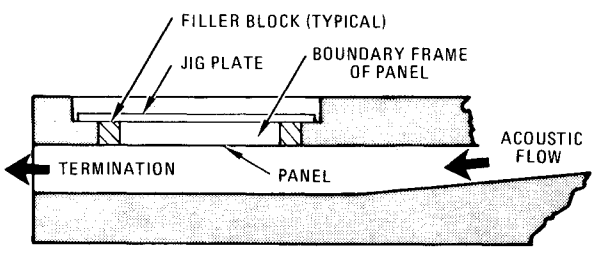

Fig. 5 Nine-bay acoustic panel and its location in the progressive wave test chamber.

Table 2 Sonic fatigue test lives and failure modes

Panel	Spectrum level "A," dB	Spectrum level "B," dB	Test life, cycles
A-1-1	140	141	4.8×10^6
A-1-2	138	–	1.2×10^6
A-2-1	139	139	4.1×10^6
A-2-2	137	–	3.4×10^6
A-3-1	140	137	3.7×10^6
A-3-2	138	–	10.5×10^6
A-4-1	141	141	2.5×10^6
A-4-2	140	–	2.5×10^6
A-5-1	140	140	6.3×10^6
A-5-2	140	–	5.3×10^6

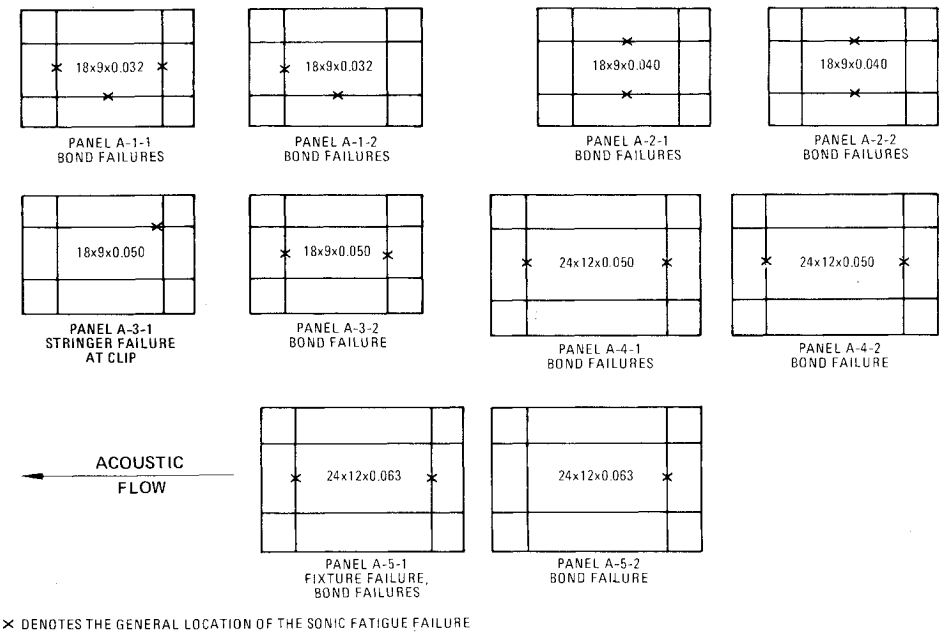

Fig. 6 Location and mode of sonic-fatigue failures.

All the damping factors listed in Table 3 were obtained under loudspeaker excitation, except for panels A-2-1 and A-3-1 for which progressive wave excitation was used. The damping factor of panel A-3-1 was obtained in the presence and in the absence of the termination box above the test panel; the variation in the damping factor of panel A-3-1 was 0.001, and resulted in the conclusion that the absence of the termination box had only an insignificant effect on the damping.

The average of the ten damping factors in Table 3 is 0.0134, whereas the average of thirty damping factors was 0.0145 with substructure riveted to the skin, reported in Table VII of Ref. 3. The difference in the average damping factors between the bonded vs riveted panels is not large. Therefore, no change in damping factor is recommended for use in sonic fatigue life predictions of bonded structures in lieu of riveted structures.

The experimental fundamental frequencies and fatigue lives of the identical pairs of panels A-2-1 and A-2-2; panels A-4-1 and A-4-2; and panels A-5-1 and A-5-2 (Tables 2 and 3) agree very well with each other. The absence of the angles on the I-section members of panel A-3-1 may have been the principal cause of the differences in modal data and the modes of fatigue failure between panels A-3-1 and A-3-2. The differences in modal data and fatigue lives between panels A-1-1 and A-1-2 may have been caused principally by the differences in the coupling of the thin (0.032-in. thickness) skins of these panels with the substructure through the adhesive bonding.

Table 3 Frequency and damping data

Panel	ζ	f_1 Hz	f_{166} Hz	$\frac{f_{166}}{f_1}$
A-1-1	0.018	137	218	1.59
A-1-2	0.015	97	204	2.10
A-2-1	0.011	144	212	1.47
A-2-2	0.009	141	211	1.50
A-3-1	0.012	165	205	1.21
A-3-2	0.011	141	207	1.47
A-4-1	0.023	80	140	1.75
A-4-2	0.009	84	144	1.71
A-5-1	0.012	103	150	1.46
A-5-2	0.014	99	143	1.44
Average	0.0134			

At the lowest overall SPL (i.e., 136 dB) used in the acoustic tests with broadband excitation, the fundamental frequency of the response was essentially the same as had been obtained in loudspeaker tests with low-level, discrete-frequency excitation. However, as the overall SPL was increased above 136 dB, the fundamental frequency of the panel increased and the rms strain response vs acoustic pressure loading relation, in general, exhibited an increasing nonlinearity. Natural frequency vs sound pressure level data are presented in Ref. 10. The increase in fundamental frequency and nonlinear strain-pressure relation are indicative of panel stiffening with increasing overall SPL that is attributed to the following factors:

1) At the lower acoustic pressures, the mean acoustic pressure is approximately zero. At the higher acoustic pressures, the mean pressure has risen significantly.

2) At the higher acoustic pressure, the unsupported skin of the central bay tends to strain extensionally significantly greater than the skin that is in contact with the adhesive at the bonded joints. Hence, an effect of the stiffeners at the high acoustic pressures is to stretch the skins and produce a net tensile (membrane) stress, which is reflected by an increasing fundamental frequency and structural stiffness of the panel, and, in particular, of the central bay.

Sonic Fatigue Life Predictions for Riveted Multibay Panels

Semiempirical equations and a nomograph[1] have been presented for predicting the stress response and sonic fatigue lives of multibay panels with the skin riveted to the substructure and subjected to acoustic excitation. The semiempirical equation for predicting stress at the center of the long side of the stiffened bay of the acoustic panel is

$$\tilde{\sigma}_S = \frac{0.072a^{1.25}S_p(f_{11})\,(b/a)^{1.75}}{h^{1.75}\zeta^{0.56}3[\,(b/a)^2+3(a/b)^2+2\,]^{0.84}}\ \text{ksi} \qquad (1)$$

The design nomograph for the riveted multibay panels based on Eq. (1) is presented in Fig. 7. In Fig. 7, a is the panel width.

Equation (1) has been applied to predict the stresses (Table 4) of acoustic test panels with spectrum levels "A" of Table 2 in the 166 dB overall SPL runs using the nominal panel lengths and widths of the central bay of the test panels (i.e., panel sizes of 18 in. × 9 in. or 24 in. × 12 in). The predicted lives for riveted aluminum panels with these geometries (Table 4) were obtained using extrapolations of Fig. 7.

Three principal differences in the dynamic behavior of bonded vs riveted multibay panels are summarized below. In general, the riveted panels are expected to fail along the line of rivets of a long side of a panel bay, whereas the bonded panels are expected to fail at the edge of the bonded joints. The use of Eq. (1) and Fig. 7 for riveted panels implies sonic fatigue failures will occur in riveted panels along the line of rivets in the center of the long side of a bay; however, the bonded acoustic test panels experienced sonic fatigue failures at the edges of the bonded joints, mainly in the center of the short sides, but also in the center of the long sides. The fundamental frequency of many of the bonded test panels (Table 3) agreed closely with predictions based on nominal dimensions of the central bay and fully clamped edge conditions, whereas the fundamental frequency of riveted test panels were shown (Fig. AV-1 of Ref. 3) to be intermediate between fully clamped and simply supported conditions. The difference in the fundamental frequencies between riveted and bonded panels may be attributed to the bonded joints producing a more effective rotational constraint to the skin because the bonded joint has a positive method (i.e., the bonding) of ensuring surface contact in the region of the joint.

Sonic Fatigue Life Predictions for the Bonded Multibay Test Panels

The sonic fatigue lives of the bonded multibay panels of this acoustic test program could have been predicted with approximately the same accuracy expected in predicting the lives of the multibay riveted panels with the use of Fig. 7 if $\bar{\sigma}_S$ in Fig. 7 were replaced by an empirically obtained factor that is called σ' such that

$$\sigma' = 0.2\bar{\sigma}_S \text{ksi} \tag{2}$$

after $\bar{\sigma}_S$ is obtained from Eq. (1). The computed stress parameter, σ', for the acoustic-test panels and the experimentally obtained sonic fatigue lives, (N), are presented in Table 5. The σ'-N data of Table 5 are presented as solid circles in Fig. 8. The dashed lines and solid line of Fig. 8 resulted from drawing the corresponding lines of Fig. 7 to a different scale and replacing the ordinate, $\bar{\sigma}_S$, with the ordinate, σ'. The computed parameter, σ', may be thought of as a stress resulting from some undefined combination of bending stress, membrane stress, and transverse shear stress.

The factor of 0.2 in Eq. (2) was obtained by a trial and error process that was performed to determine if a constant existed that would result in σ'-N data (i.e., the solid circles of Fig. 8) for the bonded panels that lie fully within the ±95% confidence limits for the riveted panels.

Table 4 Predicted sonic fatigue lives of multibay riveted panels

Test panel being simulated	$\bar{\sigma}_S$ from Eq. (1)	Predicted sonic fatigue life from Fig. 7
	ksi-rms	cycles
A-1-1	44.8	$<10^5$
A-1-2	39.3	$<10^5$
A-2-1	39.5	$<10^5$
A-2-2	31.6	$<10^5$
A-3-1	25.7	$<10^5$
A-3-2	21.4	$<10^5$
A-4-1	30.6	$<10^5$
A-4-2	43.3	$<10^5$
A-5-1	24.6	$<10^5$
A-5-2	22.5	$<10^5$

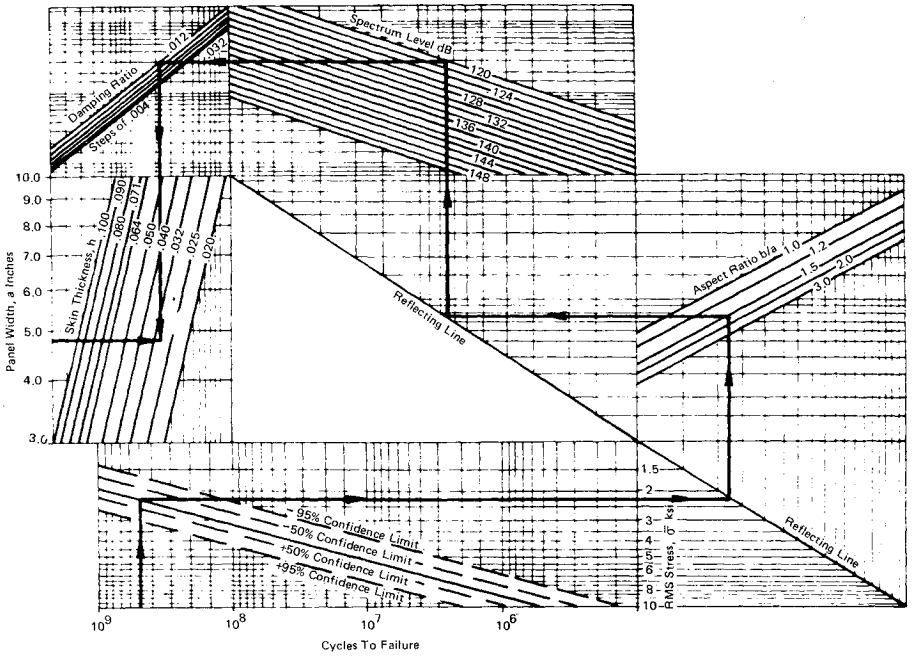

NOTE: THIS SONIC FATIGUE DESIGN NOMOGRAPH WAS DEVELOPED FOR STIFFENED ALUMINUM ALLOY PANEL SKIN WITH RIVETED JOINTS BETWEEN SKIN AND STIFFENERS AT AMBIENT TEMPERATURE (OBTAINED FROM FIGURE 5.3.1-2 OF REFERENCE 1).

Fig. 7 Sonic fatigue design nomograph for riveted multibay aluminum panels at room temperature.

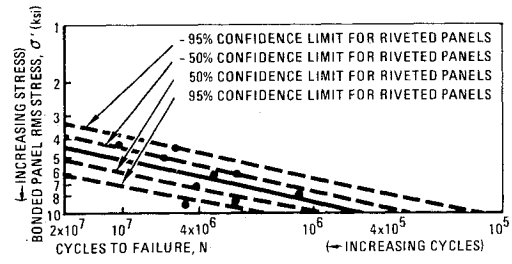

NOTES:
1. THE σ-N CURVES IN FIGURE 8 AND THE $\bar{\sigma}_S$-N CURVES IN FIGURE 7 ARE IDENTICAL (BUT DRAWN TO DIFFERENT SCALES) FOR A GIVEN CONFIDENCE LIMIT.
2. THE SOLID CIRCLES SHOWN IN THIS FIGURE DEPICT THE COMPUTED STRESS σ' AND THE SONIC FATIGUE TEST LIVES N OF THE NINE MULTIBAY PANELS THAT EXPERIENCED SONIC FATIGUE BOND FAILURES.

Fig. 8 $\sigma' - N$ relations for the bonded acoustic multibay test panels in this program.

Table 5 Acoustic panel σ'-N data

Panel	σ' from Eq. (2) ksi-rms	Experimental life (N) cycles
A-1-1	9.0	4.8×10^6
A-1-2	7.9	1.2×10^6
A-2-1	7.1	4.1×10^6
A-2-2	6.3	3.4×10^6
A-3-1	5.1	3.7×10^6 [a]
A-3-2	4.3	10.5×10^6
A-4-1	6.1	2.5×10^6
A-4-2	8.7	2.5×10^6
A-5-1	4.9	6.3×10^6
A-5-2	4.5	5.3×10^6

[a] This sonic-fatigue failure was in a simulated longeron at a clip to a simulated frame. All other sonic fatigue failures were bond failures.

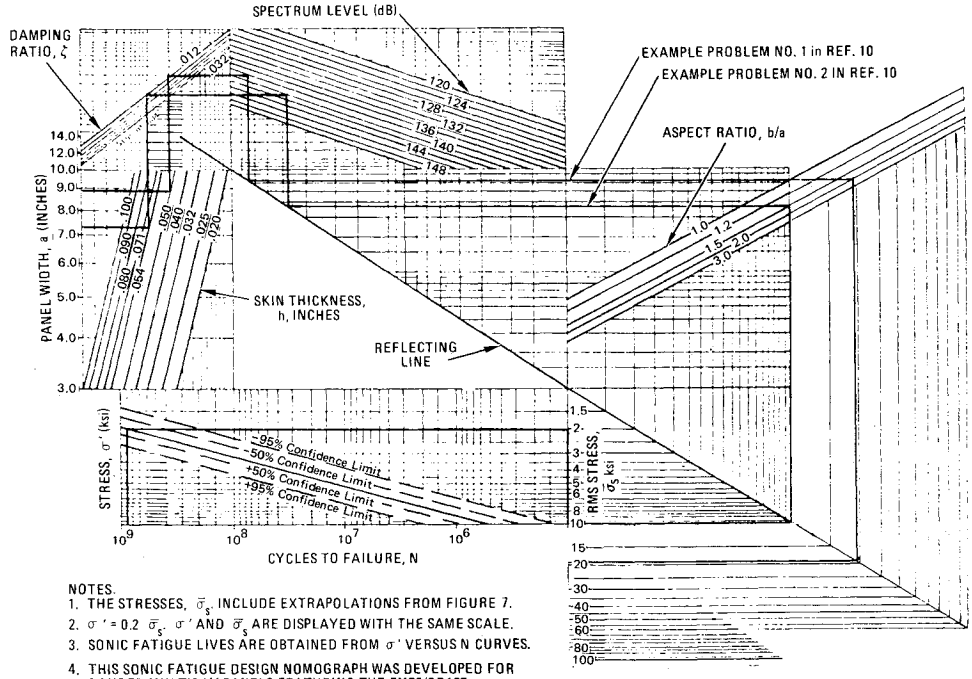

NOTES.
1. THE STRESSES, $\bar{\sigma}_S$, INCLUDE EXTRAPOLATIONS FROM FIGURE 7.
2. $\sigma' = 0.2\ \bar{\sigma}_S$. σ' AND $\bar{\sigma}_S$ ARE DISPLAYED WITH THE SAME SCALE.
3. SONIC FATIGUE LIVES ARE OBTAINED FROM σ' VERSUS N CURVES.
4. THIS SONIC FATIGUE DESIGN NOMOGRAPH WAS DEVELOPED FOR BONDED MULTIBAY PANELS FEATURING THE FM73/BR127 ADHESIVE/PRIMER SYSTEM, THE BAC-5555 SURFACE PREPARATION METHOD, AND 7075-T6 ALUMINUM ALLOY SKIN AND SUBSTRUCTURE IN A ROOM TEMPERATURE SONIC ENVIRONMENT.

Fig. 9 Sonic fatigue design nomograph for a class of bonded multibay aluminum panels.

Sonic Fatigue Design Nomograph for Bonded Panels with the FM73/BR127 Adhesive System and Phosphoric Acid Anodize Treatment

A method was developed to use the sonic fatigue design nomograph for riveted panels in Fig. 7 to predict the sonic fatigue lives of the bonded acoustic test panels of this program. The calculated parameter, σ', of Eq. (2) was postulated as the sole factor needed for predicting the sonic-fatigue bond failures. In a sense, σ' corresponds to the parameter $\bar{\sigma}_S$ in Fig. 7 for predicting the sonic fatigue lives of riveted multibay panels.

The calculated stress parameter, σ', as a function of test cycles to failure of the bonded multibay test panels were shown as solid circles in Fig. 8. Figure 9, which contains an extrapolation of the $\bar{\sigma}_S$ vs N curve of Fig. 7, was developed as a sonic fatigue design nomograph for bonded multibay test panels featuring the FM73/BR127 adhesive system, the BAC-5555 phosphoric acid anodizing process, and 7075-T6 aluminum alloy skins and substructure. The unit weight of the FM73-supported film adhesive of the acoustic test panels was 0.085 psf.

The design nomograph (using Figs. 8 and 9) is intended for use in the following manner:

1) Pick a sonic fatigue life, N;

2) Read σ' from the solid σ'-N curve in Fig. 8 or 9 (or from the upper dashed curve of Fig. 8 for more design conservatism).

3) Compute $\bar{\sigma}_S = 5\sigma'$ from Eq. (2).

4) Enter Fig. 9 with $\bar{\sigma}_S$ and determine the panel dimensions corresponding to the acoustic pressure spectrum level and panel damping factor. (The dashed lines in Figs. 8 and 9 are applicable to riveted panels of Fig. 7 and are only reference lines in Figs. 8 and 9.) Use 0.012 as a typical damping factor for the bonded panels.

Example problems illustrating the use of Fig. 9 and the four-step method that has been described in the design of a panel to be subjected to a sonic environment are given in Ref. 10.

It may appear from the application of Eqs. (1) and (2) that a riveted panel and a bonded panel will have the same sonic fatigue resistance if the thickness of the riveted panel is 2.5 times the thickness of the bonded panel. The factor of 2.5 is the constant c in the following equation:

$$\frac{\bar{\sigma}_s}{0.2\bar{\sigma}_s} = \frac{(ch_1)^{1.75}}{h_1{}^{1.75}} \tag{3}$$

Reasons that the reader should use Fig. 9 with caution and should not automatically conclude that riveted panels must be 2.5 times the thickness of bonded panels to achieve the same sonic fatigue resistance are presented in the following list.

1) The thickness and other dimensions of the riveted and bonded panels being analyzed may fall out of the range of geometrical parameters used in tests to derive Eq. (1) for riveted panels[9] and Eq. (2) for bonded panels.[10]

2) The linear strain-pressure ($\bar{\sigma}_s - S_p$) relation in Eq. (1) does not account for nonlinearities due to large deflections which may occur at high spectrum levels, e.g., 140 dB.

3) Sufficiently different shaped acoustic spectra may have an appreciable effect on the strain response and sonic fatigue lives of the test specimens. The use of Eqs. (1) and (2) imply that the acoustic spectrum level at the fundamental frequency of the panel is relatively flat and the fundamental panel mode response governs the sonic fatigue life.

4) Neither the modes nor locations of sonic fatigue failure are identified in Fig. 9.

In order to compare further the sonic fatigue resistance of bonded and riveted aluminum panels, it would be desirable to conduct a single program with structurally comparable panels except for the bonded and riveted joints.

Conclusions

A list of several important conclusions that were reached in evaluating the program results follows:

1) The sonic fatigue test lives vs spectrum level of the broadband acoustic excitation of the bonded test panels featuring the FM73/BR127 adhesive system, a phosphoric acid anodizing (BAC-5555) surface preparation treatment, and 7075-T6 aluminum alloy skins and substructure were substantially greater in almost every case than the sonic fatigue lives of riveted multibay panels of 7075-T6 aluminum alloy skins and substructure having the same skin thickness and nominal dimensions of the central bay.

2) The adaption of a well-known sonic fatigue design nomograph for riveted multibay panels (Fig. 7) resulted in a nomograph for bonded acoustic test panels (Fig. 9) with no less accuracy in predicting sonic fatigue lives.

3) More sonic fatigue test data of bonded aluminum alloy panels and failure mode identification are needed to determine the range of applicability of Fig. 9 and the effects of changes in the design configurations and thicknesses of the substructure.

4) More test data and analysis are needed to develop a predictive method for the nonlinear stress response to broadband acoustic excitation at sufficiently high intensity noise levels and the effects of the membrane stresses in the panel skins on the mode of sonic fatigue failure of bonded joints.

Acknowledgment

The activity reported herein was performed under Contract F33615-75-C-3144, "Sonic Fatigue Design Data for Bonded Aluminum Aircraft Structures," Project No. 14710130. Project engineers for this Air Force Flight Dynamics Laboratory (AFFDL) program were O. F. Maurer and C. L. Rupert. Their assistance, as well as the assistance of H. F. Wolfe of the AFFDL, is acknowledged. This program was undertaken to obtain information in support of Contract F33615-75-C-3016, "Primary Adhesively Bonded Structure Technology (PABST)," for the design and manufacture of bonded primary aircraft structure.

References

[1] Rudder Jr., F.F. and Plumblee Jr., H.E., "Sonic Fatigue Design Guide for Military Aircraft," Technical Rept. AFFDL-TR-74-112, May 1975.

[2] "Structural Design for Acoustic Fatigue," Technical Documentary Rept. No. ASD-TDR-63-820, Oct. 1963.

[3] Ballentine, J.R. et al., "Refinement of Sonic Fatigue Structural Design Criteria," Technical Rept. AFFDL-TR-67-156, Jan. 1968.

[4] Rudder Jr., F.F., "Acoustic Fatigue of Aircraft Structural Component Assemblies," Technical Rept. AFFDL-TR-71-107, Feb. 1972.

[5] Thomson, A.G.R. and Lambert, R.F., "Acoustic Fatigue Design Data," AGARDograph No. 162, Parts I, II, and III.

[6] Schneider, C.W., "Acoustic Fatigue of Aircraft Structures at Elevated Temperatures," Technical Rept. AFFDL-TR-73-155, Parts I and II, 1974.

[7] Nelson, T.F., "An Investigation of the Effects of Surrounding Structure on Sonic Fatigue," NASA CR-1536, May 1970.

[8] Rudder Jr., F.F., "Study of Effects of Design Details on Structural Response to Acoustic Excitation," NASA CR-1959, March 1972.

[9] Jacobson, M.J. and Finwall, P.E., "Effects of Structural Heating on the Sonic Fatigue of Aerospace Vehicle Structures," Technical Rept. AFFDL-TR-73-56, Jan. 1974.

[10] Jacobson, M.J., "Sonic Fatigue Design Data for Bonded Aluminum Aircraft Structures," Technical Rept. AFFDL-TR-77-45, June 1977.